scientific reports

Check for updates

OPEN

PCSK9 with a gain of function D374Y mutation aggravates atherosclerosis by inhibiting PPARα expression

Yuan feng Cui[1,2,5], Xiao cui Chen[1,2,5], Tuoluonayi Mijiti[1,2], Abidan Abudurusuli[1,2], Li hui Deng[1,2], Xiang Ma[1,3] & Bangdang Chen[1,3,4]✉

The preprotein convertase, *Bacillus subtilis* protease/kexin type 9 serine protease (PCSK9), has garnered significant attention as a potential lipid lowering and therapeutic drug target for atherosclerosis (AS). Peroxisome proliferator-activated receptor alpha (PPARα) is expressed in various tissues and has crucial roles in lipid metabolism and the inflammatory response; however, the precise impact of PCSK9 on AS progression through its regulation of PPARα remains uncertain. The present study aimed to examine the impact of introducing stable liver transduction of human derived PCSK9 with a gain of function D374Y mutation ($PCSK9^{DY}$) into systemic PPARα knockout mice ($PPAR\alpha^{-/-}$) on plasma lipid levels and AS. Enzymatic assays were employed to evaluate plasma lipid concentrations at various time points, and aortic plaque formation and the degree of inflammatory infiltration quantified. Subsequently, we validated our in vivo results using mouse primary peritoneal macrophages (MPMs). Furthermore, AAV8.2-PPARα virus vector was transduced into transgenic mice of human PCSK9(h$PCSK9^{DY}$-Tg) by tail vein, and the changes of plasma lipid level and AS were detected. $PCSK9^{DY}$ expression exacerbated symptoms of hypercholesterolemia in $PPAR\alpha^{-/-}$ mice. *En face* analysis and quantification of aortic root sections demonstrated a significant increase in aortic plaque area and inflammatory infiltration in $PCSK9^{DY}$ transduced $PPAR\alpha^{-/-}$ mice. Secretion of inflammatory cytokines was elevated in $PCSK9^{DY}$ transduced $PPAR\alpha^{-/-}$ mice. In vitro, recombinant hPCSK9 protein promotes the foam cell formation and inflammatory cytokines secretion of $PPAR\alpha^{-/-}$ MPMs by increasing the expression of SR-A and TLR4/NF-κB pathway proteins. AAV8.2-PPARα virus vector can reduce the plasma lipid level and AS formation in h$PCSK9^{DY}$-Tg mice. These finding demonstrate that $PCSK9^{DY}$ expression notably facilitated AS progression in $PPAR\alpha^{-/-}$ mice by increasing plasma lipid concentrations and inflammation. However, overexpression of PPARα can reduce AS formation in h$PCSK9^{DY}$-Tg mice.

Keywords Atherosclerosis, Lipoproteins, Proprotein convertase subtilisin/Kexin type 9 Serine protease, Peroxisome proliferator activated receptor alpha, Inflammation

Atherosclerosis (AS), the predominant cardiovascular disease, remains the primary cause of cardiovascular fatalities in developed nations[1,2]. AS is a chronic condition characterized by substantial accumulation of lipid and fibrous deposits within the lumens of major arterial vessels. Established risk factors for atherosclerosis include hypercholesterolemia, hypertension, and diabetes mellitus[3,4]. Vascular inflammation and dyslipidemia are significant contributors to AS pathogenesis, causing an increased risk of atherosclerotic cardiovascular disease development[5–7]. Therefore, gaining deeper understanding of the underlying mechanisms influencing vascular inflammation and dyslipidemia is crucial for effective AS prevention and treatment.

[1]Xinjiang Key Laboratory of Cardiovascular Disease Research, State Key Laboratory of Pathogenesis, Prevention and Treatment of High Incidence Diseases in Central Asia, Clinical Medicine Institute, First Affiliated Hospital of Xinjiang Medical University, Urumqi 830011, Xinjiang, China. [2]Basic Medical College, Xinjiang Medical University, Urumqi 830011, Xinjiang, China. [3]Department of Cardiology, First Affiliated Hospital of Xinjiang Medical University, Urumqi 830011, China. [4]Clinical Medicine Institute, First Affiliated Hospital of Xinjiang Medical University, 137 Liyushan South Road, Urumqi 830054, China. [5]Yuan feng Cui and Xiao cui Chen contributed equally to this work. ✉email: 6357@xjmu.edu.cn

Bacillus subtilis protease/kexin type 9 serine protease (PCSK9), also known as neural apoptosis regulated convertase 1 (NARC-1), is the ninth member of the proprotein convertases family, and is primarily synthesized and secreted by the liver[8,9]. Mature PCSK9 facilitates low density lipoprotein receptor (LDL-R) degradation and has crucial roles in regulating plasma LDL cholesterol (LDL-C), lipoprotein(a), and triglyceride (TG) rich lipoprotein levels, which can increase susceptibility to cardiovascular disease[10,11]. In humans, D374Y gain of function PCSK9 mutation ($PCSK9^{DY}$) is associated with elevated plasma LDL-C levels and increased susceptibility to atherosclerotic cardiovascular disease; conversely, loss of function PCSK9 mutations have the opposite effect[12–14]. Furthermore, PCSK9 overexpression in macrophages leads to heightened atherosclerotic inflammation by activating the TLR4/NF-κB pathway. In contrast, silencing PCSK9 in macrophages reduces inflammatory cytokine secretion by inhibiting the TLR4/NF-κB pathway[15].

Peroxisome proliferator activated receptor (PPAR) α, a ligand activated transcription factor, plays significant roles in inflammation, lipid metabolism, and AS[16,17]. Administration of the PPARα agonist, fenofibrate, can effectively suppress expansion of the atherosclerotic plaque area and inflammatory infiltration, while also reducing secretion of inflammatory cytokines in LDL-$R^{-/-}$ mice. Additionally, fenofibrate treatment can slow the progression of atherosclerotic lesions in ApoE and FXR double knockout mice[18,19]. Bone marrow transplantation experiments in PPARα deficient mice demonstrated that PPARα activation effectively impedes AS progression in mice[20]. Despite numerous studies on the relationship between PPARα and AS, the impact of $PCSK9^{DY}$ on acceleration of AS progression through its influence on PPARα remains unexplored.

The aim of this study was to examine the impact of $PCSK9^{DY}$ on plasma lipoprotein levels and AS in $PPARα^{-/-}$ mice, along with its potential underlying mechanisms, in a diet induced model of AS. The results revealed that $PCSK9^{DY}$ transexpression in $PPARα^{-/-}$ mice led to significant elevations of plasma and hepatic ApoB expression levels, accompanied by notable increases in plasma total cholesterol (TC), TG, LDL-C, and inflammatory cytokine levels. These changes led to enlargement of atherosclerotic plaques and intensification of inflammatory infiltration. Additionally, AAV8.2-PPARα transduction can reduce the plasma lipid level and reduce the formation of atherosclerosis in $hPCSK9^{DY}$-Tg mice.

Materials and methods

Mice and treatments

Male C57BL/6J mice (WT-13week), $PPARα^{-/-}$ mice(13week) and human $PCSK9^{D374Y}$ transgenic ($hPCSK9^{DY}$-Tg-8week) mice were obtained from the Shanghai Model Organisms Center. All animals were housed under a 12 h light-dark cycle with free access to water and food. Initially, animals were given a standard rodent diet for one week to acclimate to their new environment. First, AAV8.2-GFP (AAV-GFP) or AAV8.2-$PCSK9^{D374Y}$ (AAV-$PCSK9^{DY}$)[21], in a total volume of 200 μL containing 2×10^{11} vector genomes(vg)/mouse (WT + AAV-GFP; WT + AAV-$PCSK9^{DY}$), were injected into the tail veins of WT mice; the two groups were fed a chow diet for 6 weeks. Afterwards, AAV-GFP or AAV-$PCSK9^{DY}$ were transduced into WT and $PPARα^{-/-}$ mice, and the four groups(WT + AAV-GFP; WT + AAV-$PCSK9^{DY}$; $PPARα^{-/-}$ + AAV-GFP; $PPARα^{-/-}$ + AAV-$PCSK9^{DY}$) of mice were fed a Western diet(comprising 1.25% cholesterol, 15% lard, 5% egg yolk powder; MD12017, medicience) for 6 months[22]. In the end, AAV-GFP or AAV-PPARα virus were delivered into $hPCSK9^{DY}$-Tg mice via tail veins injection at a dose of 2×10^{11}vg/mouse ($hPCSK9^{DY}$-Tg + AAV-GFP; $hPCSK9^{DY}$-Tg + AAV-PPARα); The mice were fed a Western diet for 4 months. At the conclusion of the experiments, animals were anesthetized with a mixture of ketamine, xylazine, and atropine (100, 20, and 1.2 mg/kg, respectively, i.p.), followed by blood sample collection from the retro-orbital plexus and harvesting of heart, liver, and aorta tissues.

Ethics approval

The ethics and care of all animal experiments received approval from the Animal Care and Ethics Committees of First Affiliated Hospital of Xinjiang Medical University (Grant No:20211018-03) and the Institutional Animal Care and Use Committee of China and all methods were in accordance the relevant protocols, guidelines and regulations. All animal studies adhered to the ARRIVE 2.0 requirements, which included study design, animal numbers, randomization, and statistical methods.

Biochemical assays

At different time points post virus particle injection, blood was collected from the retro-orbital plexus. Plasma TC (WAKO, Japan), TG (WAKO, Japan), LDL-C (Nanjing Jian cheng Bioengineering Institute, China), and high-density lipoprotein cholesterol (HDL-C, Nanjing Jian cheng Bioengineering Institute, China) levels were measured enzymatically using a colorimetric diagnostic kit.

Quantitative analysis of atherosclerotic lesions

En face analysis of the entire length of the aorta and cross-sectional analysis of the proximal aorta were conducted to assess aortic atherosclerotic lesions. For *en face* analysis, aortas from different groups were longitudinally excised from the heart to the iliac arteries and stained with Oil Red O. Each stained aorta was photographed using a Canon digital camera (Tokyo, Japan). The percentage of the lesion area to the corresponding whole aortic area represented the atherosclerotic degree of each group.

Aortic roots were immediately embedded in optimal cutting temperature (OCT) compound after harvest and stored at − 80 °C for cryo-sectioning. Serial sections of OCT-embedded aortas were cut using a cryostat at an 8 μm thickness from the aortic valve. Root sections were then stained with Oil Red O or antibodies against CD68 (AbD Serotec). Lesion areas were measured using Image Pro Plus software and are presented as $μm^2$.

Cell culture and treatments

Mouse primary peritoneal macrophages (MPMs) were isolated as previously described[23]. Briefly, 8–10 week WT or PPARα$^{-/-}$ mice were intraperitoneally injected with 1 ml of 3% thioglycolate. MPMs were harvested via peritoneal lavage 4 days later and cultured in DMEM supplemented with 15% FBS and 1% penicillin/streptomycin. Cells were then cultured with ox-LDL (50 μg/ml) for 24 h, after which hPCSK9 (1 μg/ml) (HY-P70545, MCE) or PBS were added to the cultured cells for an additional 24 h.

Intracellular lipid deposition

MPMs were stained with Oil Red O to evaluate intracellular fat content. Cells were washed with PBS, fixed with 4% paraformaldehyde, and stained with Oil Red O solution for 30 min. Subsequently, cells were washed with PBS and visualized using an inverted microscope (Leica, Germany). Quantitative analysis of lipid content was performed by 75% alcohol extraction after Oil Red O staining, and absorbance was measured at 492 nm using a microplate reader. Cellular cholesterol levels were measured using a colorimetric assay kit (Nanjing Jiancheng Bioengineering Institute, China).

Cytokine enzyme linked immunosorbent assay (ELISA)

Plasma and cell supernatant concentrations of IL-1β were assayed using an ELISA kit (Cloud-Clone Corp, China). Plasma concentrations of hPCSK9 (R&D, USA) and ApoB (Abcam, UK) were also determined using ELISA kits, following the manufacturer's protocols.

Real-time quantitative RT-PCR

Total RNA was isolated from tissues using Trizol reagent (Invitrogen, USA) and stored at − 80°C. cDNAs were synthesized using a First-Strand Synthesis System (TIANGEN, China), followed by real-time PCR using Power SYBR® Green PCR Master Mix (Applied Biosystems). Amplification, detection, and data analysis were performed using a 7500 PCR system (Applied Biosystems). Fold changes in relative gene expression were determined using the $2^{-\Delta\Delta CT}$ method, with *18S* as the internal control. The following primers were used for amplifying: 18S, 5'-TTGACGGAAGGGCACCACCAG-3' (forward) and 5'-GCACCACCACCCACGGAATCG-3' (reverse); and PPARα, 5'-AGCTGGTGCTAGCCTTGCGTTC-3' (forward) and 5'-AGACATGCAGGATCTTGGTGAG-3' (reverse).

Western blot analysis

Total protein samples were extracted from cells and murine tissues, as previously described[24]. Primary antibodies targeting PCSK9 (Novus, NB300-959), PPARα (Cayman, 101710), ApoB (Meridian, K23300R), LDL-R (abcam, ab52818), SR-A (abcam, ab151707), ABCA1 (Novus, NB400-145), ABCG1 (Novus, NB400-132), TLR4 (PTM BIO, PTM5192), IκBα (CST, 4812), NF-κB P65 (CST, 8242), NF-κB phosphor-P65 (CST, 4148), GFP(CST, 2307)and GAPDH (abcam, ab8245) were used. Immunoreactive protein bands were detected using an ECL kit (Millipore) and quantified using Image Lab 4.0 software (Bio-Rad, USA).

Statistical analysis

Data are presented as mean ± standard error of the mean, unless otherwise specified. Statistical comparisons between two groups were conducted using the unpaired Student's *t* test. When comparisons involved more than two groups, analyses were performed by two way ANOVA followed by Tukey's correction. Statistical comparisons were conducted using GraphPad Prism software. In all experiments, P values < 0.05 were considered statistically significant.

Results

PCSK9^{DY} transexpression reduced hepatic PPARα protein abundance in WT mice

WT mice were fed a chow diet and tail vein transduced with AAV-GFP or AAV-PCSK9^{DY} virus vectors for 6 weeks. Plasma ELISA results indicated a significant release of PCSK9 protein into the bloodstream in PCSK9^{DY} transduced WT mice (Fig. 1A). Body weight analysis showed no significant difference between GFP and PCSK9^{DY} infected mice. At 6 weeks post injection, plasma TC and TG levels in PCSK9^{DY} expressed mice were 1.69 and 1.19-fold higher, respectively, than those in GFP injected controls (65.90 ± 3.11 versus 176.98 ± 15.54 mg/dL; 80.52 ± 6.71 versus 176.06 ± 17.22 mg/dL; Fig. 1A). Tail vein injection of WT mice with 2×10^{11} viral particles resulted in stable PCSK9 protein expression in the liver, measured after 6 weeks (Fig. 1B). Consistent with these results, lower hepatic LDL-R protein and higher PCSK9 protein levels than those in controls were detected in PCSK9^{DY} transexpression mice (Fig. 1B). In WT mice, PCSK9^{DY} expression led to decreased hepatic PPARα protein levels; this decrease was modest but significant (0.30-fold). Consistent with its effect on PPARα protein expression, PCSK9^{DY} expression also significantly decreased hepatic PPARα mRNA expression by 0.33-fold (Fig. 1B). These results suggest that PCSK9^{DY} may regulate dyslipidemia and AS by reducing PPARα expression. Thus, we constructed PPARα systemic knockout mice, to further investigate whether PCSK9^{DY} affects plasma lipid and AS in mice by regulating PPARα.

PCSK9^{DY} expression significantly exacerbates hyperlipidemia in PPARα$^{-/-}$ mice

WT and PPARα$^{-/-}$ mice were injected with AAV-GFP or AAV-PCSK9^{DY} virus, and fed a Western diet for 6 months. At 6 months post injection, plasma hPCSK9 was detected using an ELISA kit. The results revealed that PCSK9^{DY} injection significantly increased plasma hPCSK9 protein levels in both WT and PPARα$^{-/-}$ mice (Fig. 2A). Analysis of mouse body weight showed that neither GFP nor PCSK9^{DY} transduction significantly influenced WT or PPARα$^{-/-}$ mouse. Hepatic overexpression of GFP or PCSK9^{DY}was validated by significant increases in GFP and PCSK9 protein levels (Fig. 2B). Hepatic levels of LDL-R protein were almost completely

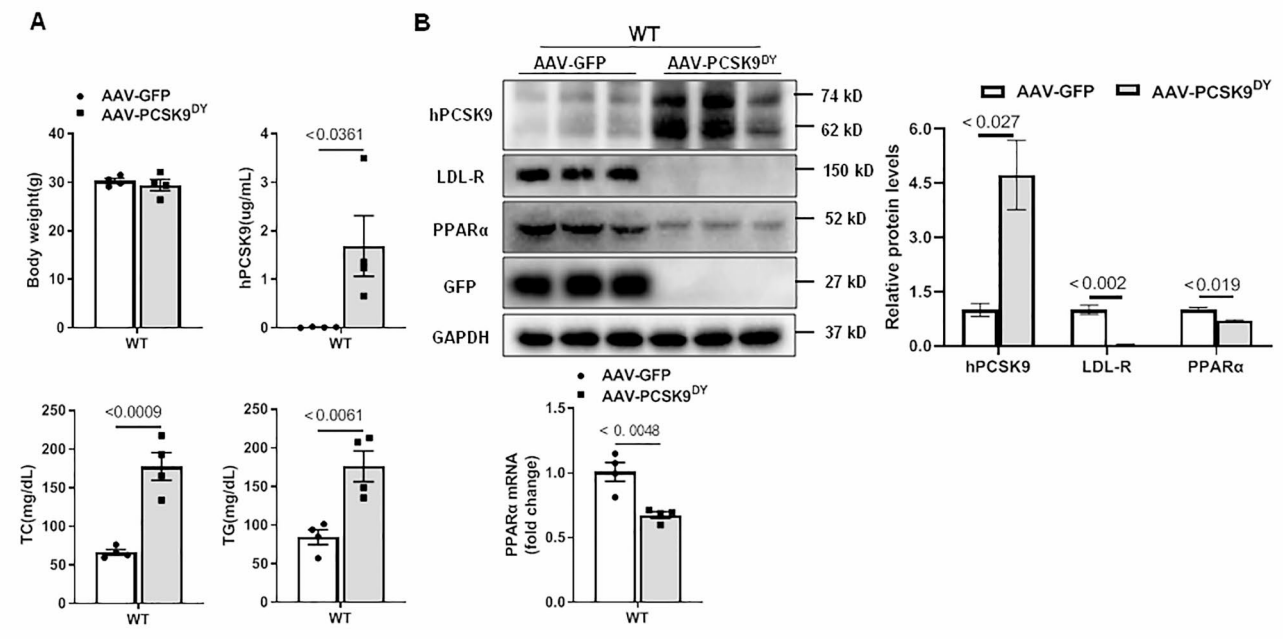

Fig. 1. Expression of PCSK9^{DY} reduces hepatic PPARα abundance in WT mice when fed a chow diet. (**A**) Body weight, serum levels of human PCSK9 protein, total cholesterol(TC), triglyceride(TG) in WT mice injected with AAV-PCSK9^{DY} or AAV-GFP virus particles($n = 4$). (**B**) Hepatic hPCSK9, GFP, LDL-R and PPARα protein levels of AAV-PCSK9^{DY} transduced WT mice are analyzed by western blot and normalized to GAPDH, and then were presented relative to the level in AAV-GFP control($n = 3$). Real-time PCR analysis of PPARα mRNA in mouse liver 6 weeks after injection of AAV-PCSK9^{DY} virus. PPARα mRNA amounts are normalized to 18s mRNA and are presented relative to the level in WT animals($n = 4$). Data are presented as the mean ± SEM. Unpaired Student's *t*-test was used.

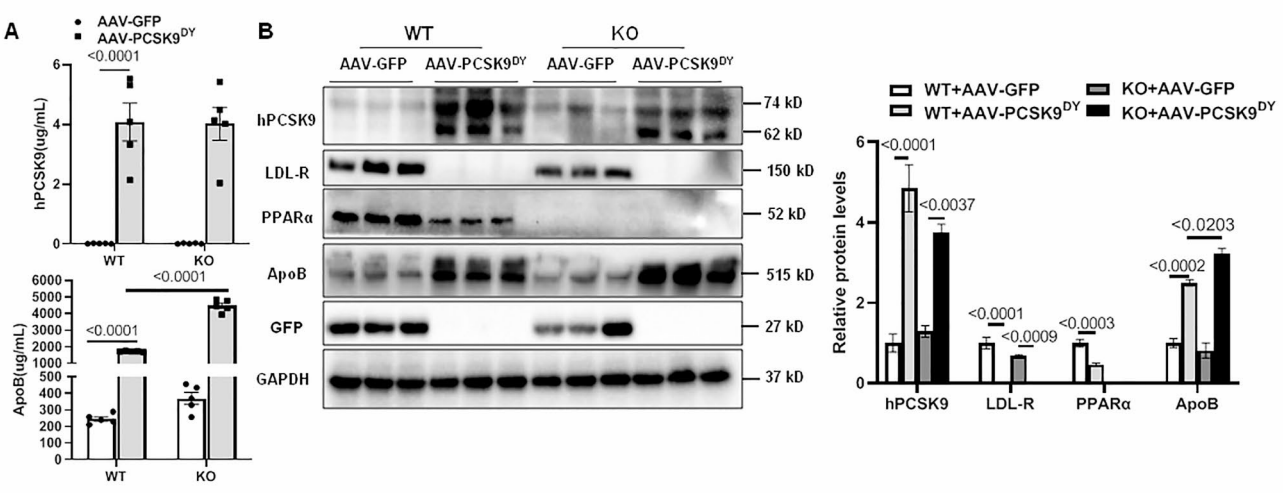

Fig. 2. PPARα deficiency exacerbates AAV-PCSK9^{DY} induced hyperlipidemia on fed a Western diet. (**A**) Plasma hPCSK9 and ApoB concentrations in four group mice($n = 5$). (**B**) Hepatic hPCSK9, LDL-R, PPARα, ApoB and GFP protein were determined by Western blot on lysates from snap frozen tissue harvested on 6 months, and normalized to GAPDH, and then were presented relative to the level in AAV-GFP injected WT control ($n = 3$). Data are presented as the mean ± SEM. Statistical comparisons were performed by two way ANOVA with Tukey correction for multiple comparisons.

eliminated in PCSK9^{DY} transduced WT and PPARα$^{-/-}$ mice (Fig. 2B). After 6 months, PPARα protein expression in the livers of PCSK9^{DY} injected WT mice was 0.54 fold lower than that in GFP injected controls (Fig. 2B). Interestingly, WT mice injected with PCSK9^{DY} showed a marked increase in hepatic ApoB protein expression (Fig. 2B). Furthermore, hepatic ApoB expression was significantly increased in PCSK9^{DY} transduced PPARα$^{-/-}$

mice relative to WT mice (Fig. 2B). Consistent with these results, plasma ApoB levels were significantly increased by 5.99 fold in PCSK9^{DY} transduced WT mice compared with GFP injected controls (Fig. 2A). Further, PPARα$^{-/-}$ mice transduced with PCSK9^{DY} exhibited plasma ApoB levels 1.60 fold higher than those in PCSK9^{DY} injected WT mice (Fig. 2A).

Next, plasma lipid concentrations were assessed using plasma samples from all groups collected at baseline (day 0), 2 weeks, 1 and 2 months post infection. At day 0, all groups exhibited similar baseline plasma TC, TG, and LDL-C levels (Table 1). At 2 weeks post injection, plasma levels of TC and LDL-C in PCSK9^{DY} expressing WT mice were significantly increased by 2.19 fold and 2.15 fold, respectively, relative to GFP injected WT mice. These differences were maintained 2 months after injection (Table 1). Interestingly, plasma TC, TG, and LDL-C levels in PCSK9^{DY} transduced PPARα$^{-/-}$ mice were almost 1.42, 4.14 and 1.32 fold higher than those in similarly injected WT mice (Table 1). Similarly, these differences were sustained through to 2 months (Table 1). These results demonstrate that PCSK9^{DY} expression led to significantly increased plasma TC, TG, and LDL-C levels in WT mice, with more pronounced effects observed in PPARα$^{-/-}$ mice.

PCSK9^{DY} transduction significantly promotes atherogenesis and inflammatory infiltration in PPARα$^{-/-}$ mice

En face aortic and aortic sinus plaque areas were examined in four groups of mice using Oil Red O staining. Remarkably, in WT mice, PCSK9^{DY} infection led to larger plaque areas in aortas and aortic roots compared to GFP transduction Fig. 3A&B). Histological analysis of aortas and aortic roots plaques in PPARα$^{-/-}$ mice indicated that the atherosclerotic lesion areas with PCSK9^{DY} expression were larger than those in WT mice Fig. 3A&B). Furthermore, immunohistochemical staining of aortic roots was conducted to assess the presence of markers of inflammatory macrophages (CD68) in all groups of mice Fig. 3B). The results revealed that inflammatory infiltration of the aortic sinus was higher in the PCSK9^{DY} group relative to the GFP group of WT mice. Similarly, regarding lesion areas, inflammatory infiltration of the aortic root in PCSK9^{DY} transduced PPARα$^{-/-}$ mice exhibited a significant increase relative to the PCSK9^{DY} expressing WT group Fig. 3B). These findings indicate that PCSK9^{DY} led to substantial atherosclerotic plaque lesion area expansion and a notable increase in inflammatory infiltration within the aortic sinus of PPARα$^{-/-}$ mice.

PCSK9^{DY} expression regulates inflammatory cytokine secretion through activation of the TLR4/NF-κB pathway and enhances SR-A protein expression in PPARα$^{-/-}$ mice

To explore the possible mechanisms by which PCSK9^{DY} expression influences inflammation and aortic plaque lesion extent in PPARα$^{-/-}$ mice, we measured the levels of inflammatory cytokines in plasma via ELISA and assessed the expression levels of aortic SR-A, cholesterol transport proteins, and proteins in the TLR4/NF-κB pathway in four groups by western blot. ELISA analysis showed that the plasma IL-1β levels in PCSK9^{DY} transduced WT mice were significantly higher (3.34 fold) than those in GFP transduced WT mice (Fig. 4A). Further, IL-1β secretion was significantly higher (0.76 fold) in PCSK9^{DY} injected PPARα$^{-/-}$ mice than that in corresponding WT mice (Fig. 4A). Moreover, expression levels of TLR4, phosphorylated P65 protein, and IκBα proteins were higher in PCSK9^{DY}expressing mice than those in GFP inoculated WT mice (Fig. 4B&C). Interestingly, PCSK9^{DY} transduced PPARα$^{-/-}$ mice had significantly higher levels of these proteins than corresponding WT mice (Fig. 4B&C). Similarly, SR-A protein expression was significantly increased in WT mice after PCSK9^{DY} transduction compared with that in GFP inoculated controls. SR-A protein levels were clearly higher in PCSK9^{DY} transduced PPARα$^{-/-}$ mice than those in equivalent WT mice (Fig. 4B&C). No significant changes in levels of ABCA1 and ABCG1 were detected in any group (Fig. 4B&C). These results suggest that PCSK9^{DY} markedly increases inflammatory cytokine secretion and aortic inflammation through activation of the TLR4/NF-κB pathway. Additionally, PCSK9^{DY} increases aortic plaque area, likely by promoting lipid uptake through upregulation of the scavenger receptor, SR-A.

Recombinant hPCSK9 protein promotes foam cell formation and SR-A expression in primary peritoneal macrophages from PPARα$^{-/-}$ mice

MPMs from WT and PPARα$^{-/-}$ mice were isolated and cultured. MPMs from WT mice were analyzed by immunofluorescence using the macrophage marker, CD68, which indicated that the vast majority of cells were macrophages (Fig. 5A). Next, MPMs from WT and PPARα$^{-/-}$ mice were stimulated with ox-LDL, followed by treatment with recombinant hPCSK9 protein or PBS, and then stained for lipid content and quantified. Oil Red O staining and quantification revealed that recombinant hPCSK9 protein promoted foam cell formation in WT MPMs compared with the control group (Fig. 5B&C). Further, recombinant hPCSK9 protein significantly enhanced foam cell formation in PPARα$^{-/-}$ MPMs compared with WT MPMs (Fig. 5B&C). Additionally, cellular cholesterol content in all groups showed consistent results on Oil Red O quantification (Fig. 5C). To delineate the mechanism by which recombinant hPCSK9 protein increases foam cell formation in PPARα$^{-/-}$ MPMs, the expression of scavenger receptors and cholesterol transporters was determined. The results showed that recombinant hPCSK9 protein significantly increased SR-A expression in WT MPMs compared with the control, but barely affected the expression of cholesterol transporters, including ABCA1 and ABCG1 (Fig. 5D). Furthermore, SR-A expression in recombinant hPCSK9 protein treated PPARα$^{-/-}$ MPMs was higher than in equivalent WT MPMs. Consistent with these results, we did not observe any significant changes in ABCA1 and ABCG1 expression (Fig. 5D). The above findings suggest that recombinant hPCSK9 protein may lead to an increase in the number of foamy macrophages by up-regulating SR-A levels in PPARα$^{-/-}$ MPMs, without altering expression of the transporter proteins, ABCA1 and ABCG1.

	TC(mg/dL)				TG(mg/dL)				LDL-C(mg/dL)			
	0d	2w	1 m	2 m	0d	2w	1 m	2 m	0d	2w	1 m	2 m
a($n=6$)	77.01 ± 2.55	149.03 ± 2.75	143.66 ± 2.55	156.80 ± 4.14	95.22 ± 8.79	92.55 ± 8.45	93.98 ± 3.60	103.24 ± 12.84	48.71 ± 2.32	58.37 ± 3.47	64.56 ± 1.16	65.33 ± 2.70
b($n=5$)	71.56 ± 1.20	474.79 ± 22.51$^{\#}$	514.56 ± 45.63$^{\#}$	471.90 ± 41.28$^{\#}$	95.75 ± 9.78	100.03 ± 6.94	120.87 ± 13.54	136.91 ± 9.93	51.03 ± 0.77	184.02 ± 10.82$^{\#}$	259.79 ± 14.30$^{\#}$	163.91 ± 23.19$^{\#}$
c($n=6$)	71.09 ± 3.22	115.33 ± 16.42	119.78 ± 16.34	111.07 ± 15.52	89.40 ± 2.40	90.79 ± 3.43	102.90 ± 4.75	111.25 ± 8.95	49.87 ± 1.16	58.76 ± 3.86	65.72 ± 3.47	68.81 ± 6.18
d($n=6$)	73.12 ± 4.68	1150.04 ± 36.96*	1408.31 ± 24.99*	1262.24 ± 46.04*	91.73 ± 5.59	514.37 ± 44.91*	528.63 ± 50.72*	509.03 ± 61.86*	48.32 ± 1.54	427.58 ± 47.16*	394.71 ± 15.85*	342.14 ± 25.51*

Table 1. Changes of Circulating TC、TG and LDL-C in four groups of mice. a: WT + AAV-GFP; b:WT + AAV-PCSK9^{DY}; c: PPARα$^{-/-}$ + AAV-GFP; d:PPARα$^{-/-}$ + AAV-PCSK9^{DY}; $^{\#}P < 0.05$, b vs. a;$^{*}P < 0.05$, d vs. b. lipids levels in the plasma collected at different time point were determined, and statistical analysis was performed using two way ANOVA followed by Tukey's correction. Data shown are mean ± SEM.

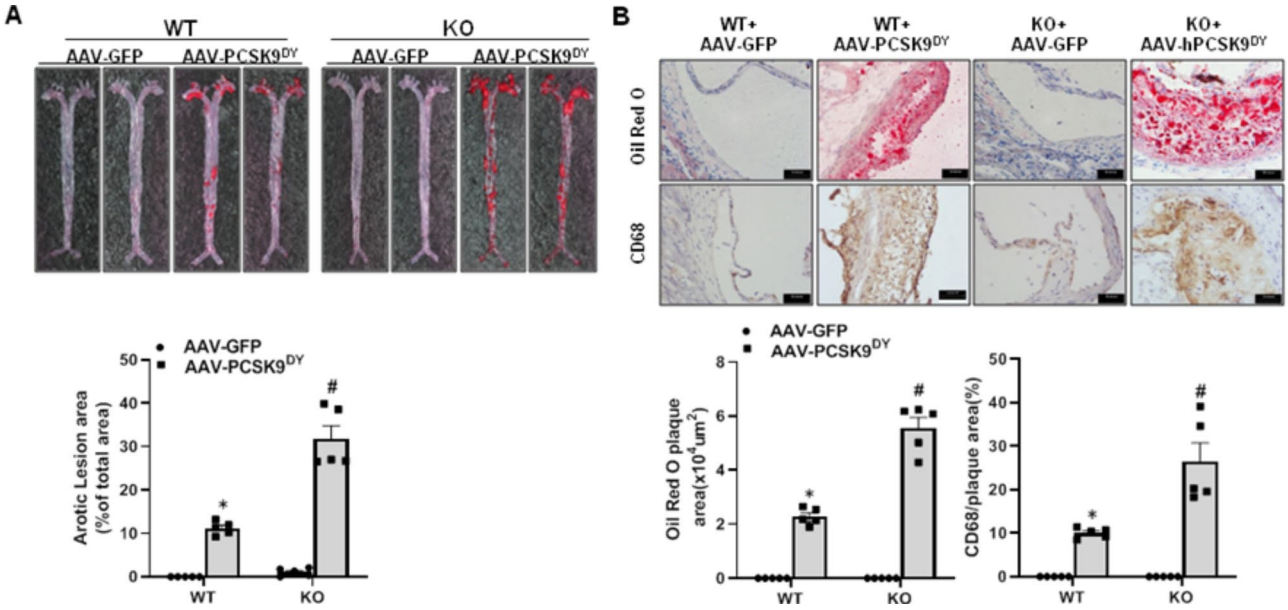

Fig. 3. PPARα ablation exacerbates AAV-PCSK9^{DY} induced atherosclerosis and inflammatory infiltration. (**A**) Whole aortas stained with Oil Red O for *en face* analysis of plaque area. Quantification of the mean aortic lesion area in each group as a percentage of the mean aortic area($n = 5$). (**B**) Representative microphotographs of the Oil Red O and CD68 stained aortic roots sections from the WT and PPARα$^{-/-}$ mice that were injected AAV-PCSK9^{DY} or AAV-GFP virus particles at 40×magnification. Quantification of lesion area and CD68 positive area of aortic root ($n = 5$). Data are presented as the mean ± SEM. Statistical comparisons were performed by two way ANOVA with Tukey correction for multiple comparisons.

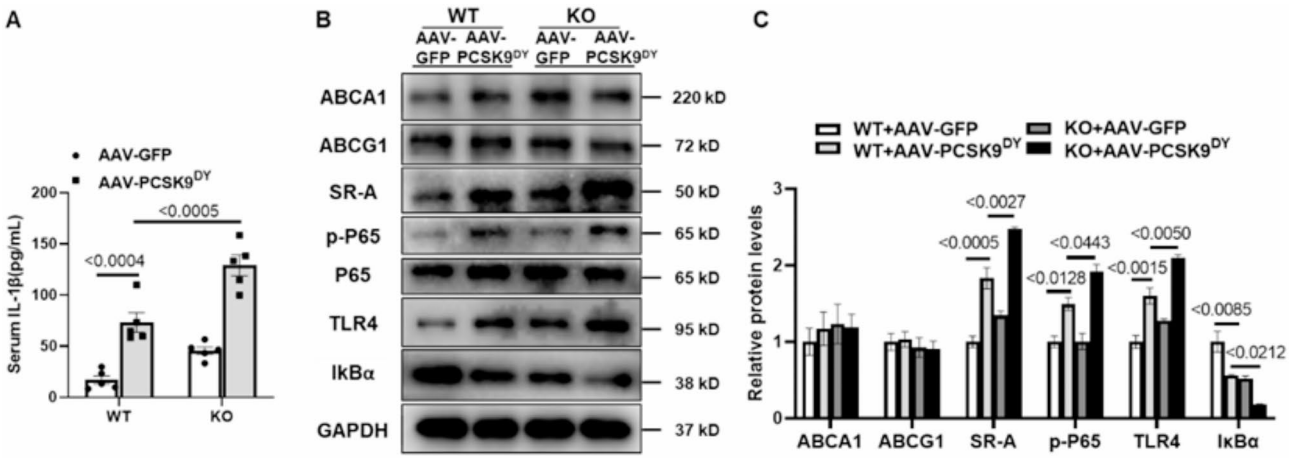

Fig. 4. PCSK9^{DY} expression regulates inflammatory cytokine secretion involving activation of the TLR4/NF-κB pathway and enhances protein expression levels of scavenger receptor in PPARα$^{-/-}$ mice. (**A**) Serum levels of IL-1β was detected via ELISA($n = 5$). (**B**) ABCA1, ABCG1, SR-A, p-P65, TLR4 and IκBα protein levels in atherosclerotic aortas of WT and PPARα$^{-/-}$ mice injected AAV-GFP or AAV-PCSK9^{DY} virus particles. (**C**) Quantitative results of these protein levels of (B) relative to GAPDH($n = 3$). Data are presented as the mean ± SEM. Statistical comparisons were performed by two way ANOVA with Tukey correction for multiple comparisons.

Recombinant hPCSK9 protein enhances ox-LDL induced inflammatory responses to PPARα$^{-/-}$ in MPMs

To further investigate the role of hPCSK9 in inflammation regulation and the potential underlying mechanisms, we selected ox-LDL stimulated MPMs as a cell model. Levels of IL-1β in cell supernatants were significantly higher in recombinant hPCSK9 protein treated WT MPMs than those in control cells (Fig. 6A); however, IL-1β levels were higher in recombinant hPCSK9 protein treated PPARα$^{-/-}$ MPMs than those in WT MPMs (Fig. 6A). In addition, recombinant hPCSK9 protein promoted ox-LDL induced up-regulation of TLR4 and p-P65 proteins

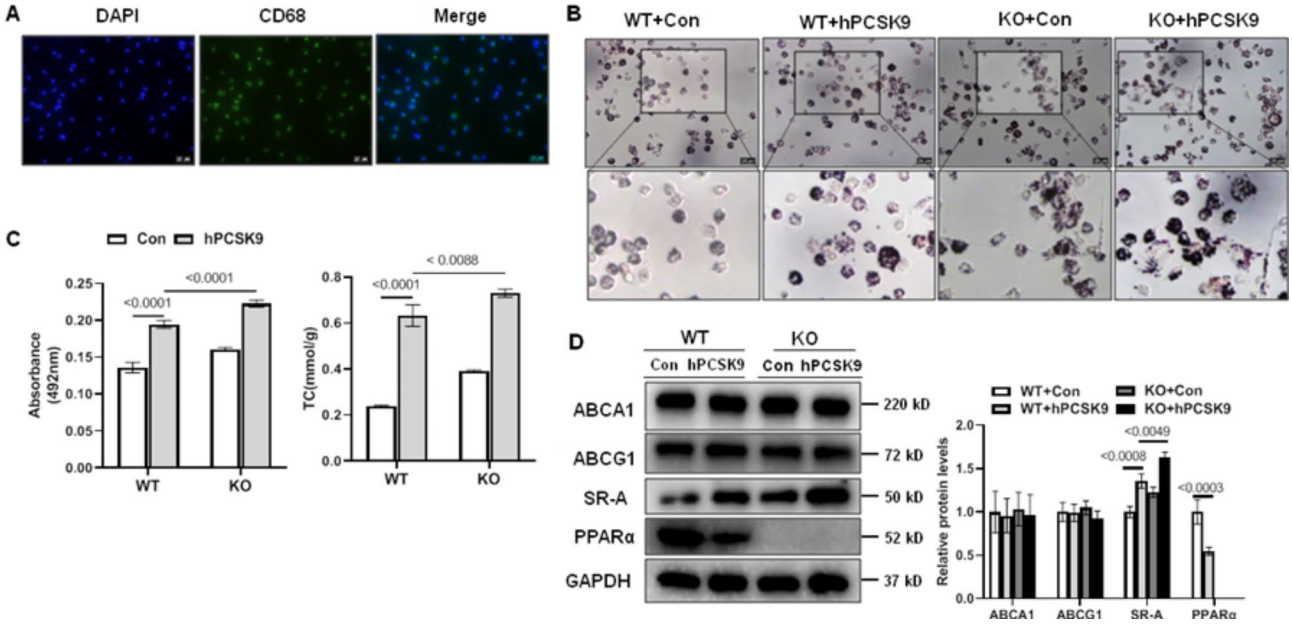

Fig. 5. Recombinant hPCSK9 protein promotes ox-LDL-induced foam cell formation and scavenger receptor expression in MPMS of PPARα$^{-/-}$. (**A**) MPMs were isolated and identified by immunofluorescence using the macrophage marker CD68. (**B**) Oil Red O staining analysis of foam cell formation at 40× magnification. (**C**) Quantitative results of foam cell formation were obtained by measuring the eluted oil red O dye at 492 nm using a thermos spectrophotometer. Levels of cellular cholesterol was analyzed in MPMs($n = 3$). (**D**) Determination of ABCA1, ABCG1, SR-A, PPARα levels in MPMs($n = 3$). Data are presented as the mean ± SEM. Statistical comparisons were performed by two-way ANOVA with Tukey correction for multiple comparisons.

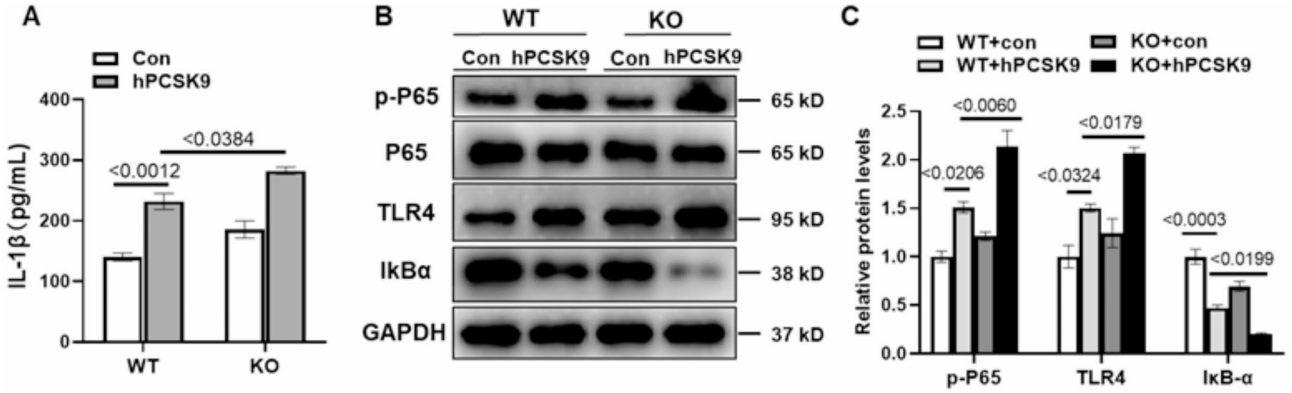

Fig. 6. Recombinant hPCSK9 protein enhances ox-LDL induced inflammatory response in MPMs of PPARα$^{-/-}$. (**A**) IL-1β protein level was detected via ELISA in MPMs($n = 3$). (**B**) TLR4, IκBα, p-P65 protein expression were detected via Western blot in MPMs. (**C**) Quantitative results of these protein levels of (**B**) ($n = 3$). Data are presented as the mean ± SEM. Statistical comparisons were performed by two-way ANOVA with Tukey correction for multiple comparisons.

in WT MPMs, while the expression of TLR4 and p-P65 proteins was higher in hPCSK9 treated PPARα$^{-/-}$ MPMs (Fig. 6B&C). Moreover, recombinant hPCSK9 protein accelerated ox-LDL induced IκBα degradation in WT MPMs, and significantly enhanced this effect in PPARα$^{-/-}$ MPMs (Fig. 6B&C). These data confirm that recombinant hPCSK9 protein can enhance an inflammatory response involving activation of the TLR4/NF-κB pathway in PPARα$^{-/-}$ MPMs.

AAV-PPARα attenuates dyslipidaemia and AS formation in hPCSK9^{DY}-Tg mice

Given that PCSK9^{DY} overexpression reduces PPARα expression, we assessed whether overexpression of PPARα reduces dyslipidemia and AS formation. AAV-PPARα was transduced into hPCSK9^{DY}-Tg mice by tail vein, and compared with AAV-GFP, the plasma lipid level and AS formation of mice were detected. The results showed

	hPCSK9^{DY}-Tg + AAV-GFP($n = 5$)	hPCSK9^{DY}-Tg + AAV-PPARα($n = 5$)
Body weight(g)	42.34 ± 1.95	41.12 ± 1.19
hPCSK9(ug/ml)	8.02 ± 0.63	8.78 ± 0.51
TC(mg/dL)	1133.99 ± 107.35	775.95 ± 25.85*
TG(mg/dL)	320.69 ± 33.81	212.11 ± 8.89*
LDL-C(mg/dL)	456.18 ± 16.62	375.38 ± 17.01*
HDL-C(mg/dL)	151.54 ± 26.67	184.02 ± 18.55
ApoB(ug/ml)	3291.24 ± 273.69	2245.99 ± 276.94*
IL-1β(pg/ml)	208.50 ± 5.08	169.17 ± 7.02*

Table 2. Changes of body weight, blood lipid level, Circulating hPCSK9, ApoB and IL-1β. Body weight, lipids levels, hPCSK9 and cytokines in the plasma collected at the end of the study were determined, and statistical analysis was performed using Unpaired Student's *t* tests. $^{*}P < 0.05$,Data shown are mean ± SEM.

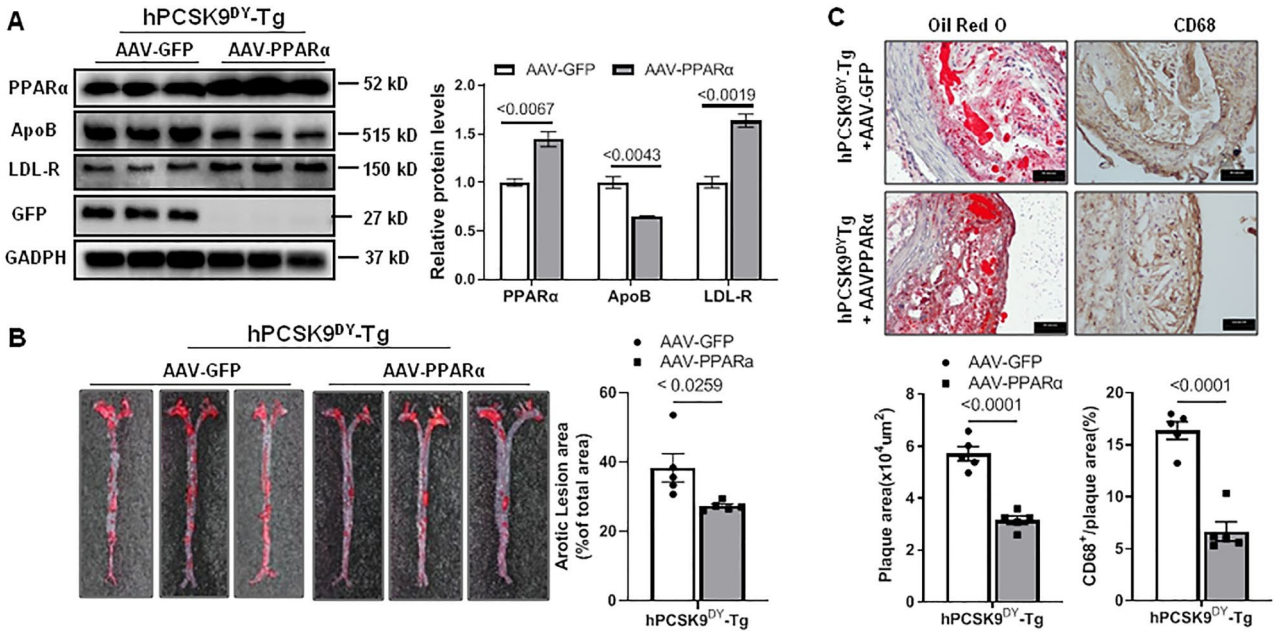

Fig. 7. PPARα overexpression attenuates AS formation in hPCSK9^{DY}-Tg mice. (**A**) Hepatic PPARα, ApoB and LDL-R protein levels of AAV-PPARα transduced hPCSK9^{DY}-Tg mice are analyzed by western blot and normalized to GAPDH, and then were presented relative to the level in AAV-GFP control($n = 3$). (**B**) Whole aortas stained with Oil Red O for en face analysis of plaque area. Quantification of the mean aortic lesion area in each group as a percentage of the mean aortic area($n = 5$). (**C**) Representative microphotographs of the Oil Red O and CD68 stained aortic roots sections from the hPCSK9^{DY}-Tg mice that were injected AAV-PPARα or AAV-GFP virus particles at 40×magnification. Quantification of lesion area and CD68 positive area of aortic root ($n = 5$).Data are presented as the mean ± SEM. Unpaired Student's *t* test was used.

that the circulating TC, TG, LDL-C, ApoB and IL-1β levels in the hPCSK9^{DY}-Tg + AAV-GFP group were reduced by 0.17, 0.44, 0.18, 0.32 and 0.19 folds, respectively, compared with those in the hPCSK9^{DY}-Tg + AAV-PPARα group(Table 2). However, there was no statistical difference in body weight, circulating hPCSK9 and HDL-C levels between the two groups of mice.

It was further found that the protein expression of hepatic PPARα and LDLR increased 0.97-fold and 0.64-fold, respectively, in the hPCSK9^{DY}-Tg + AAV-PPARα group compared with the hPCSK9^{DY}-Tg + AAV-GFP group; however, the ApoB protein expression decreased 0.42-fold (Fig. 7A). In addition, compared with AAV-GFP group, the plaque area of aorta and aortic sinus in AAV-PPARα group decreased by 0.28 and 0.45 folds respectively, while the inflammatory infiltration of macrophages decreased by 0.62 folds(Fig. 7B&C). Together, these results indicate that PPARα overexpression ameliorates dyslipidaemia and reduces AS formation in hPCSK9^{DY}-Tg mice.

Discussion

The primary novel finding of this study is that PCSK9^{DY} transduction significantly inhibited PPARα protein, resulting in substantial increases in plasma TC and LDL-C levels, accompanied by an increase in atherosclerotic

plaque area. Expression of PCSK9^{DY} in PPARα-/- mice resulted in hyperlipidemia formation and increased atherosclerotic plaque area, which may be due to elevated plasma apolipoprotein B and LDL-C levels. Furthermore, the underlying mechanism appears to involve upregulation of SR-A by PCSK9^{DY} transduction, as well as activation of TLR4/NF-κB signaling, contributing to plaque lesion area enlargement and inflammatory responses in aortic tissue. Finally, to some extent, PPARa overexpression can reduce the atherosclerotic area of transgenic mice with hPCSK9^{DY}.

Since its initial identification as a genetic factor associated with familial hypercholesterolemia, PCSK9 has undergone rapid development as a potential target for novel lipid lowering medications currently undergoing clinical testing or already approved[10,12,25]. Notably, PCSK9 gain of function mutations substantially elevate the risk of hyperlipidemia and atherosclerotic disease. However, PCSK9 loss of function mutations have the opposite effect. In *db/db* mice fed a high fat diet, mouse PCSK9^{D377Y} overexpression leads to a significant elevation of plasma TC and TG, as well as a notable increase in atherosclerotic plaque lesion area[26]. Human PCSK9^{D374Y} gain of function mutations have similar effects. Previous studies have found that overexpression of PCSK9^{D374Y} in ApoE-/- mice and PCSK9^{D374Y} transgenic mice exhibited significantly elevated plasma TC, TG, and ApoB levels, as well as a significant increase in atherosclerotic plaque area[22,27]. Conversely, administration of PCSK9 monoclonal antibody can reduce plasma TC and TG levels in ApoE$^{-/-}$ mice, while also leading to a reduction in atherosclerotic plaque lesion area[28]. In addition, it was found in 2022 that after overexpression of PCSK9^{D377Y}, the expression of PPARα gene in mouse liver decreased and the area of atherosclerotic plaque increased[29]. On the contrary, studies have shown that inhibiting PCSK9 can promote the conversion of cholesterol by activating PPARα-mediated CYP7A1 expression[30]. These studies show that PPARα plays an important role in the dyslipidemia regulated by PCSK9 ^{D377Y}. So does PPARα also play an important role in the dyslipidemia regulated by human PCSK9^{D374Y}?

In the current investigation, we observed that PCSK9^{DY} inoculation led to notable elevations in plasma TC and TG levels, while concurrently inducing a substantial reduction in hepatic PPARα protein expression levels in WT mice fed a chow diet. Consequently, it is plausible that PCSK9^{DY} may influence dyslipidemia and AS progression in mice by modulating PPARα protein expression.

Hypercholesterolemia is a major risk factor for atherosclerotic cardiovascular disease, significantly raising the risk of myocardial infarction and mortality. PCSK9 gain of function mutations directly contribute to a substantial elevation in plasma LDL-C levels, which, in turn, correlates positively with AS development. ApoB, a pivotal component of LDL-C, plays a crucial role in the assembly and secretion of TG-rich lipoproteins and lipid transport[31]. PCSK9^{D374Y} significantly increases plasma TC, LDL-C, and ApoB levels, leading to a marked rise in atheromatous plaque lesion area[22,27]. Similarly, PPARα has a vital role in regulating plasma lipid levels. Fenofibrate, a PPARα agonist, is commonly used clinically for dyslipidemia treatment and lipid lowering[32]. Relevant studies showed that plasma TC and LDL-C levels were considerably higher in PPARα$^{-/-}$ mice than those in WT mice[33]. In high fat diet fed liver specific PPARα knockout mice, the levels of plasma TC, TG and ApoB increased significantly[34]. Additionally, related research demonstrated that the PPARα agonist, GW7674, could reduce LDL fractions in LDL-R$^{-/-}$ mice[35]. These results show that PPARα plays an important role in blood lipid level and atherosclerosis. In western diet, our results reveal that PCSK9^{DY} transduced WT mice had substantially increased plasma levels of TC, LDL-C, and ApoB, accompanied by a significant increase in aortic plaque area, relative to controls transduced with GFP. Furthermore, PCSK9^{DY} transexpression in PPARα$^{-/-}$ mice led to significantly higher plasma TC, TG, LDL-C, and ApoB levels, along with increased aortic plaque area, relative to that observed in corresponding WT mice. The prominent increase in plasma LDL-C levels in PCSK9^{DY} transduced PPARα$^{-/-}$ mice may be attributable to their markedly elevated hepatic and plasma ApoB protein levels, and serve as the primary driver of AS exacerbation.

Chronic inflammation is widely acknowledged to be a hallmark of atherosclerotic cardiovascular disease, playing a pivotal role in the initiation, progression, and rupture of atherosclerotic plaques[36]. The inflammatory cytokine, IL-1β, is abundantly expressed in atherosclerotic lesions, accelerating vascular inflammation and AS progression[37]. Related research results show that PCSK9 is closely related to the secretion of IL-1β[38]. Moreover, Numerous studies have emphasized the connection between PCSK9 and atherosclerotic inflammation. Previous studies have found that recombinant PCSK9 protein significantly increased IL-1β, IL-6, TNF-α, CXCL2, and MCP1 mRNA levels in THP-1 and human primary macrophages, with this proinflammatory effect primarily dependent on LDL-R[39]. Furthermore, PCSK9 overexpression in ApoE$^{-/-}$ mice and RAW264.7 macrophages activated the TLR4/NF-κB pathway, resulting in increased secretion of the proinflammatory cytokines, IL-1β and TNF-α, in plasma and cell supernatants. Conversely, PCSK9 silencing reduced proinflammatory cytokine secretion and diminished inflammatory infiltration of plaques[15]. A study of Arya et al. highlighted that PCSK9 monoclonal antibody treatment reduced aortic tissue TLR2 and NF-κB levels, along with plasma TNF-α and IL-6 levels, providing more effective suppression of vasculitis[40]. Additionally, it is found that PCSK9 silencing in THP-1 cells mitigated ox-LDL stimulated inflammatory responses by inhibiting the NF-κB pathway[40]. Studies have also shown that recombinant PCSK9 protein increased SR-A expression in mouse macrophages treated with ox-LDL and promoted inflammatory cytokines secretion in TNF-α treated mouse macrophages[41]. PPARα also plays a crucial role in atherosclerotic inflammation, and PPARα agonists reduce plaque area, inhibit NF-κB pathway activity, decrease macrophage foam cell formation, and suppress inflammatory cytokines secretion[35,42,43]; however, few studies have investigated whether PCSK9^{DY} influences AS progression by regulating PPARα. Our results demonstrate that PCSK9^{DY} significantly promotes inflammatory cytokine secretion, in both plasma and cell culture supernatants of MPMs from PPARα$^{-/-}$ mice. Mechanistic studies in MPMs revealed that recombinant hPCSK9 protein expression substantially increased TLR4 expression, inducing NF-κB pathway activation. Hence, TLR4/NF-κB activation may underlie inflammatory cytokines secretion and heightened inflammatory infiltration in the aortic sinus. Additionally, SR-A was significantly upregulated in recombinant hPCSK9 protein treated PPARα$^{-/-}$ MPMs, with unchanged protein expression levels of ABCA1 and ABCG1;

this upregulation of SR-A may be the primary reason for the marked increase in foam cells, a key component of atherosclerotic plaques.

A study found that feeding hPCSK9^{DY}-Tg mice a western diet significantly increased circulating TC, LDL-C, and ApoB levels and led to the rapid formation of AS plaque lesions that were similar in size to those of LDL-R$^{-/-}$ mice, suggesting that the hPCSK9^{DY}-Tg mice are a type of mice capable of spontaneous AS lesion formation[44]. Tail vein transduction of AAV-PPARα resulted in significantly more hepatic PPARα protein expression in mice, indicating successful overexpression of the recombinant AAV-PPARα vector. It was further found that plasma lipid levels and AS lesion area were decreased in AAV-PPARα overexpressing mice. The reason why AAV-PPARα leads to the decrease of AS formation in hPCSK9^{DY}-Tg mice may be closely related to the decrease of circulating ApoB and LDL-C level.

The current study sheds new light on the elevated inflammatory infiltration and increased atherosclerotic plaque area observed in PPARα$^{-/-}$ mice following PCSK9^{DY} transduction; however, it is crucial to acknowledge the limitations and shortcomings of the investigation when interpreting the findings. First, the precise cause of the substantial elevation in plasma cholesterol and TG in PPARα$^{-/-}$ mice after PCSK9^{DY} transduction remains unknown. Second, although atherosclerotic plaque area and aortic sinus inflammatory infiltration were significantly elevated in PCSK9^{DY} transduced PPARα$^{-/-}$ mice, the mechanism by which PCSK9^{DY} regulates PPARα to influence these aspects remains unclear.

In conclusion, in this study we investigated the impact of PCSK9^{DY} transduction on plasma lipid concentrations and AS lesion in PPARα$^{-/-}$ mice. Administration of a Western diet and tail vein injection of PCSK9^{DY} led to significant rises in plasma lipoproteins, atherosclerotic plaque area, and inflammatory infiltration levels in PPARα$^{-/-}$ mice. Further exploration revealed that PCSK9^{DY} expression may enhance plasma lipoprotein levels by increasing plasma and hepatic ApoB expression. Moreover, PCSK9^{DY} contributed to amplified atherosclerotic plaque area and inflammatory infiltration by upregulating SR-A receptors in the aorta and MPMs, as well as by promoting Toll4/NF-κB pathway activation. Finally, PPARα overexpression can reduce the plasma lipid level and AS formation in hPCSK9^{DY}-Tg mice. The precise mechanism by which PCSK9^{DY} transexpression influences plasma levels in PPARα$^{-/-}$ mice, particularly whether it solely involves the action of lipoprotein ApoB or if other mechanisms are at play, remains unclear. Additionally, the molecular mechanism by which PCSK9^{DY} regulates PPARα to impact AS progression, and whether this regulation is dependent on LDL-R, requires further in depth investigation in future studies.

Data availability

Data is provided within the manuscript or supplementary information files.

Received: 8 September 2024; Accepted: 18 February 2025
Published online: 26 February 2025

References

1. Weber, C. et al. Atherosclerosis: current pathogenesis and therapeutic options. *Nat. Med.* **17** (11), 1410–1422 (2011).
2. Raskob, G. E. et al. Thrombosis: a major contributor to global disease burden. *Arterioscler. Thromb. Vasc Biol.* **34** (11), 2363–2371 (2014).
3. Ding, Z. et al. PCSK9 and inflammation: role of shear stress, pro-inflammatory cytokines, and LOX-1. *Cardiovasc. Res.* **116** (5), 908–915 (2020).
4. Libby, P. The changing landscape of atherosclerosis. *Nature* **592** (7855), 524–533 (2021).
5. Li, H. et al. Hepatic cholesterol transport and its role in non-alcoholic fatty liver disease and atherosclerosis. *Prog Lipid Res.* **83**, 101109 (2021).
6. Baratta, F. et al. Nonalcoholic fatty liver disease and fibrosis associated with increased risk of cardiovascular events in a prospective study. *Clin. Gastroenterol. Hepatol.* **18** (10), 2324–2331 (2020).
7. Tousoulis, D. et al. Inflammatory cytokines in atherosclerosis: current therapeutic approaches. *Eur. Heart J.* **37** (22), 1723–1732 (2016).
8. Benjannet, S. et al. NARC-1/PCSK9 and its natural Mutants: Zymogen cleavage and effects on the low density lipoprotein (LDL) receptor and LDL cholesterol. *J. Biol. Chem.* **279** (47), 48865–48875 (2004).
9. Ragusa, R. et al. PCSK9 and atherosclerosis: looking beyond LDL regulation. *Eur. J. Clin. Invest.* **51** (4), e13459 (2021).
10. Yurtseven, E. et al. An update on the role of PCSK9 in atherosclerosis. *J. Atheroscler Thromb.* **27** (9), 909–918 (2020).
11. Xia, X. D. et al. Regulation of PCSK9 expression and function: mechanisms and therapeutic implications. *Front. Cardiovasc. Med.* **8**, 764038 (2021).
12. Abifadel, M. et al. Mutations in PCSK9 cause autosomal dominant hypercholesterolemia. *Nat. Genet.* **34** (2), 154–156 (2003).
13. Denis, M. et al. Gene inactivation of proprotein convertase subtilisin/kexin type 9 reduces atherosclerosis in mice. *Circulation* **125** (7), 894–901 (2012).
14. Zhao, Z. et al. Molecular characterization of loss-of-function mutations in PCSK9 and identification of a compound heterozygote. *Am. J. Hum. Genet.* **79** (3), 514–523 (2006).
15. Tang, Z. H. et al. New role of PCSK9 in atherosclerotic inflammation promotion involving the TLR4/NF-κB pathway. *Atherosclerosis* **262**, 113–122 (2017).
16. Issemann, I. et al. Activation of a member of the steroid hormone receptor superfamily by peroxisome proliferators. *Nature* **347** (6294), 645–650 (1990).
17. Islinger, M. et al. Be different–the diversity of peroxisomes in the animal Kingdom. *Biochim. Biophys. Acta.* **1803** (8), 881–897 (2010).
18. Lee, Y. et al. The effects of Ppar agonists on atherosclerosis and nonalcoholic fatty liver disease in ApoE-/-FXR-/- mice. *Endocrinol. Metab. (Seoul).* **36** (6), 1243–1253 (2021).
19. Li, A. C. et al. Peroxisome proliferator-activated receptor gamma ligands inhibit development of atherosclerosis in LDL receptor-deficient mice. *J. Clin. Invest.* **106** (4), 523–531 (2000).
20. Zandbergen, F. et al. PPARαlpha in atherosclerosis and inflammation. *Biochim. Biophys. Acta.* **1771** (8), 972–982 (2007).
21. Chen, B. D. et al. Targeting transgene to the heart and liver with AAV9 by different promoters. *Clin. Exp. Pharmacol. Physiol.* **42** (10), 1108–1117 (2015).

22. Tavori, H. et al. Human PCSK9 promotes hepatic lipogenesis and atherosclerosis development via apoE- and LDLR-mediated mechanisms. *Cardiovasc. Res.* **110** (2), 268–278 (2016).
23. Layoun, A. et al. Isolation of murine peritoneal macrophages to carry out gene expression analysis upon Toll-like receptors stimulation. *J. Vis. Exp.* **98**, e52749 (2015).
24. Sun, M. H. et al. Cardioprotective effects of constitutively active MEK1 against H_2O_2-induced apoptosis and autophagy in cardiomyocytes via the ERK1/2 signaling pathway. *Biochem. Biophys. Res. Commun.* **512** (1), 125–130 (2019).
25. Reyes-Soffer, G. et al. Effects of PCSK9 Inhibition with Alirocumab on lipoprotein metabolism in healthy humans. *Circulation* **135** (4), 352–362 (2017).
26. Xu, M. et al. A novel mouse model of diabetes, atherosclerosis and fatty liver disease using an AAV8-PCSK9-D377Y injection and dietary manipulation in *Db/db* mice. *Biochem. Biophys. Res. Commun.* **622**, 163–169 (2022).
27. Herbert, B. et al. Increased secretion of lipoproteins in Transgenic mice expressing human D374Y PCSK9 under physiological genetic control. *Arterioscler. Thromb. Vasc Biol.* **30** (7), 1333–1339 (2010).
28. Ason, B. et al. PCSK9 Inhibition fails to alter hepatic LDLR, Circulating cholesterol, and atherosclerosis in the absence of ApoE. *J. Lipid Res.* **55** (11), 2370–2379 (2014).
29. Mobilia, M. et al. Dennd5b-Deficient mice are resistant to PCSK9-Induced hypercholesterolemia and Diet-Induced hepatic steatosis. *J. Lipid Res.* **63** (12), 100296 (2022).
30. Chen, Z. et al. Inhibition of PCSK9 prevents and alleviates cholesterol gallstones through PPARα-mediated CYP7A1 activation. *Metabolism* **152**, 155774 (2024).
31. Gavish, D. et al. Heritable allele-specific differences in amounts of ApoB and low-density lipoproteins in plasma. *Science* **244** (4900), 72–76 (1989).
32. Goldfine, A. B. et al. Fibrates in the treatment of dyslipidemias–time for a reassessment. *N Engl. J. Med.* **365** (6), 481–484 (2011).
33. Montagner, A. et al. Liver PPARα is crucial for whole-body fatty acid homeostasis and is protective against NAFLD. *Gut* **65** (7), 1202–1214 (2016).
34. Stec, D. E. et al. Loss of hepatic PPARα promotes inflammation and plasma hyperlipidemia in diet-induced obesity. *Am. J. Physiol. Regul. Integr. Comp. Physiol.* **317** (5), R733–R745 (2019).
35. Li, A. C. et al. Differential Inhibition of macrophage foam-cell formation and atherosclerosis in mice by PPARαlpha, beta/delta, and gamma. *J. Clin. Invest.* **114** (11), 1564–1576 (2004).
36. Punnanithinont, N. et al. Anti-inflammatory therapies in Atherosclerosis - Where are we going? *Curr. Atheroscler Rep.* **27** (1), 19 (2024).
37. Libby, P. Interleukin-1 beta as a target for atherosclerosis therapy: biological basis of cantos and beyond. *J. Am. Coll. Cardiol.* **70** (18), 2278–2289 (2017).
38. Ding, Z. et al. NLRP3 inflammasome via IL-1β regulates PCSK9 secretion. *Theranostics* **10** (16), 7100–7110 (2020).
39. Ricci, C. et al. PCSK9 induces a pro-inflammatory response in macrophages. *Sci. Rep.* **8** (1), 2267 (2018).
40. Tang, Z. et al. PCSK9 SiRNA suppresses the inflammatory response induced by OxLDL through Inhibition of NF-κB activation in THP-1-derived macrophages. *Int. J. Mol. Med.* **30** (4), 931–938 (2012).
41. Ding, Z. et al. PCSK9 regulates expression of scavenger receptors and ox-LDL uptake in macrophages. *Cardiovasc. Res.* **114** (8), 1145–1153 (2018).
42. Duez, H. et al. Reduction of atherosclerosis by the peroxisome proliferator-activated receptor alpha agonist Fenofibrate in mice. *J. Biol. Chem.* **277** (50), 48051–48057 (2002).
43. Marx, N. et al. PPARαlpha activators inhibit tissue factor expression and activity in human monocytes. *Circulation* **103** (2), 213–219 (2001).
44. Luo, Y. et al. Function and distribution of Circulating human PCSK9 expressed extrahepatically in Transgenic mice. *J. Lipid Res.* **50** (8), 1581–1588 (2009).

Author contributions

Bang dang Chen conceived the present study; Yuan feng Cui and Xiao cui Chen designed the experiments and wrote the draf of the manuscript; Bang dang Chen gave the revise suggestion for this manuscript; Tuoluonayi•Mijiti and Abidan•Abudurusuli collected data; Yuan feng Cui and Xiao cui Chen performed statistical analyses; Li hui Deng, Tuoluonayi•Mijiti and Abidan•Abudurusuli collected samples and undertook laboratory experiments; Xiang Ma and Bang dang Chen supervised this study. All authors reviewed the manuscript.

Funding

This work was supported by the National Natural Science Foundation of China (U1903304, 82160169, 82460175), the Key Program of Natural Science Foundation of Xinjiang Uygur Autonomous Region (2022D01D16), Tianshan Innovative Research Team Plan (2024D14011) and Xinjiang Uygur Autonomous Region Tianshan Youth Science and Technology Elite Talent Project (2022TSYCCX0031, 2023TSYCQNTJ0027).

Declarations

Competing interests

The authors declare no competing interests.

Additional information

Supplementary Information The online version contains supplementary material available at https://doi.org/10.1038/s41598-025-91061-5.

Correspondence and requests for materials should be addressed to B.C.